Published in final edited form as:
NMR Biomed. 2019 June ; 32(6): e4085. doi:10.1002/nbm.4085.

Localized rest and stress human cardiac creatine kinase reaction kinetics at 3 tesla

William T Clarke[1,2,*], **Mark A Peterzan**[1], **Jennifer J Rayner**[1], **Rana A Sayeed**[3], **Mario Petrou**[3], **George Krasopoulos**[3], **Hannah A Lake**[4], **Betty Raman**[1], **William D Watson**[1], **Pete Cox**[5], **Moritz J Hundertmark**[1], **Andrew P Apps**[1], **Craig A Lygate**[4], **Stefan Neubauer**[1], **Oliver J Rider**[1,**], and **Christopher T Rodgers**[1,6,**]

[1]Oxford Centre for Clinical Magnetic Resonance Research (OCMR), Division of Cardiovascular Medicine RDM, University of Oxford, Level 0, John Radcliffe Hospital, Oxford, OX3 9DU, UK

[2]Wellcome Centre for Integrative Neuroimaging, FMRIB, University of Oxford, John Radcliffe Hospital, Oxford, OX3 9DU, UK

[3]Department of Cardiothoracic Surgery, John Radcliffe Hospital, Oxford University Hospitals NHS Foundation Trust, Oxford, OX3 9DU, UK

[4]Department of Cardiovascular Medicine, University of Oxford, Wellcome Trust Centre for Human Genetics, Roosevelt Drive, Oxford OX3 7BN, UK

[5]Department of Physiology Anatomy, University of Oxford, Parks Road, Sherrington Building, Oxford OX1 3PT, UK

[6]Wolfson Brain Imaging Centre, University of Cambridge, Box 65, Cambridge Biomedical Campus, Cambridge, CB2 0QQ, UK

Abstract

Purpose—Changes in the kinetics of the creatine kinase (CK) shuttle are sensitive markers of cardiac energetics but are typically measured at rest and in the prone position. This study aims to measure CK kinetics during pharmacological stress at 3T, with measurement in the supine position. A shorter “stressed saturation transfer” (StreST) extension to the triple repetition time saturation transfer (TRiST) method is proposed. We assess scanning in a supine position and validate the MR measurement against biopsy assay of CK activity. We report normal ranges of stress CK forward rate (k_f^{CK}) for healthy volunteers and obese patients.

Theory and Methods—TRiST measures k_f^{CK} in 40 minutes at 3T. StreST extends the previously developed TRiST to also make a further k_f^{CK} measurement during <20min of dobutamine stress. We test our TRiST implementation in skeletal muscle and myocardium in both prone and supine positions. We evaluate StreST in the myocardium of six healthy volunteers and 34 obese subjects. We validated MR-measured k_f^{CK} against biopsy assays of CK activity.

* To whom correspondence should be addressed, William T. Clarke, Wellcome Centre for Integrative Neuroimaging, FMRIB, Level 0, John Radcliffe Hospital, Oxford, OX3 9DU. UK. william.clarke@ndcn.ox.ac.uk, Tel: 01865 610475.
** Joint Senior Authors

Europe PMC Funders Author Manuscripts

Results—TRiST k_f^{CK} values matched literature values in skeletal muscle (k_f^{CK} = 0.25±0.03 s^{-1} vs 0.27±0.03 s^{-1}) and myocardium when measured in the prone position (0.32±0.15 s^{-1}), but a significant difference was found for TRiST k_f^{CK} measured supine (0.24±0.12 s^{-1}). This difference was due to different respiratory- and cardiac-motion-induced B_0 changes in the two positions. Using supine TRiST, cardiac k_f^{CK} values for normal-weight subjects were 0.15±0.09s^{-1} at rest and 0.17±0.15s^{-1} during stress. For obese subjects k_f^{CK} was 0.16±0.07s^{-1} at rest and 0.17±0.10 s^{-1} during stress. Rest myocardial k_f^{CK} and CK activity from LV biopsies of the same subjects correlated (R=0.43, p=0.03).

Conclusion—We present an independent implementation of TRiST on the Siemens platform using a commercially available coil. Our extended StreST protocol enables cardiac k_f^{CK} to be measured during dobutamine-induced stress in the supine position.

Keywords

^{31}P magnetic resonance spectroscopy; cardiac; creatine kinase; energy metabolism; high-energy phosphate; phosphorus; saturation transfer; TRiST; StreST

Introduction

The rate and flux of the creatine kinase (CK) exchange mechanism have been shown to be sensitive measures of heart failure(1), which is a prevalent and burdensome disease (2,3). The rate can be characterised by the pseudo first-order forward rate constant, k_f^{CK}. Phosphorus magnetic resonance spectroscopy (^{31}P-MRS) enables non-invasive measurement of myocardial k_f^{CK} (4). In addition to measuring k_f^{CK} in myocardium at rest, measuring k_f^{CK} during pharmacologically-induced stress would enable us to understand the effect of a perturbed CK mechanism in the stressed human heart (1,5).

Schär et al introduced the triple repetition time saturation transfer (TRiST) sequence to measure CK kinetics by ^{31}P-MRS at 3T (6). A TRiST acquisition lasts 40 min (out of complete protocol totalling 84 min); it measures k_f^{CK} in a one-dimensional coronal stack of slices covering the heart and chest wall (7). 1D-localised k_f^{CK} measurement during inotropic stress was achieved by Weiss et al at 1.5 T using the four-angle saturation transfer (FAST) and the derived “FASTest” method (1,4). However, FAST and FASTest rely on small-angle adiabatic pulses, which are not achievable at 3T due to radiofrequency power requirements, power deposition and T_2 relaxation (8). The 3T TRiST protocol offers an established measurement technique which can be included in a larger cardiac ^{1}H MR protocol on the same scanner. Whilst 7T ^{31}P-MRS has been used for 3D-localised k_f^{CK} measurements, the existing published methods have long duration and the higher field strength restricts the recruitment of subjects who have undergone surgical procedures (9).

An increase in myocardial work can be reliably maintained, without physical exercise (and therefore motion), by administering dobutamine intravenously. However, the duration of intravenous infusion should be kept to a minimum length. Current guidelines prescribe 15 minute stress protocols(10) and they recommend patients should be scanned in the supine position, for safety in case of arrhythmia. Measuring k_f^{CK} within this timeframe is currently only possible using the “Two repetition time saturation transfer” (TwiST) method, published

during the course of this study (7). However, although TwiST assumes a fixed phosphocreatine (PCr) intrinsic longitudinal relaxation time (T_1*) i.e. in the hypothetical case of PCr not undergoing chemical exchange, it is not yet known whether T_1* remains constant in clinically-relevant groups; e.g. obese, normal-weight, and heart failure.

We therefore propose to perform stress k_f^{CK} measurements at 3T in two steps: first, derive a per-subject baseline PCr T_1* with TRiST; and second, performing two further scans during dobutamine-induced stress to record the stress k_f^{CK} in less than 20 minutes of dobutamine infusion. This stress saturation-transfer (StreST) protocol yields a stack of 1D-localised k_f^{CK} measurements at rest *and stress*. We describe below the implementation of StreST and validate the underlying TRiST method in skeletal muscle, in human myocardium in the prone position and subsequently in the supine position, where we correlate surgical left ventricular (LV) biopsy-obtained CK activity against pre-operative myocardial k_f^{CK} in a set of within-patient paired measurements. We then demonstrate StreST by using it to record normative ranges of rest *and stress* k_f^{CK} in the myocardium of normal volunteers and in older obese and age-matched control cohorts.

Theory

CK regenerates adenosine triphosphate (ATP) from PCr according to the equilibrium expression $PCr^{2-} + MgADP^{-} + H^{+} \rightleftharpoons Cr + MgATP^{2-}$. CK provides the temporal energy reserve in muscle. TRiST uses steady-state saturation of the terminal (γ) phosphate-group of ATP to measure k_f^{CK}, the pseudo first-order rate constant of the CK reaction in the forward (ATP-generating) direction. Since the ^{31}P nuclei in PCr and γ-ATP are undergoing two-site exchange, continuous saturation of γ-ATP allows the forward exchange rate constant to be determined using

$$k_f^{CK} = \frac{1}{T_1'}\left(1 - \frac{M'_{PCr}}{M_{PCr}^{Ctrl}}\right). \quad [1]$$

Table 1 summarises each parameter's physical meaning. TRiST measures T_1', M'_{PCr} and M_{PCr}^{Ctrl}. This requires three steps: two to measure M'_{PCr} and T_1' using the dual-TR method(8), and a third to measure M_{PCr}^{Ctrl} (see Figure 1).

The intrinsic longitudinal relaxation time T_1^*, can be computed from(11)

$$T_1^* = T_1' \frac{M_{PCr}^{Ctrl}}{M'_{PCr}}. \quad [2]$$

Therefore, by substituting Eq. [2], Eq. [1] may be recast in terms of T_1^* rather than T_1' (4):

$$k_f^{CK} = \frac{1}{T_1^*}\left(\frac{M_{PCr}^{Ctrl}}{M'_{PCr}} - 1\right). \quad [3]$$

T_1^* is a hypothetical longitudinal relaxation constant for a molecule without chemical exchange. Assuming that T_1^* does not change from one scan to the next (e.g. in myocardium at rest vs under stress), then an additional measurement of k_f^{CK} may be made in two steps: measuring M_{PCr}^{Ctrl} and M'_{Pcr}. This is a similar assumption to that used in the "FASTer"/"FASTest" adaptation of the FAST method (4).

StreST protocol

Our new "StreST" protocol comprises a rest measurement of k_f^{CK} and PCr T_1* using TRiST (four steps) and a measurement of k_f^{CK} during intravenous pharmacological stress (two additional steps). The six (4+2) steps are given in Table 2. All steps are completed in a single scanning session.

In future studies using the proposed StreST protocol, subjects will be scanned in the supine position, instead of the prone position used in the original TRiST studies. Prone scanning is considered to be unsafe for a cardiac monitoring perspective, especially when scanning patients with heart failure who may be at greater risk of dangerous arrhythmia. 1/400 patients receiving dobutamine experience a life-threatening arrhythmia (12).

Methods

All subjects were recruited in a manner approved by the local research ethics committee. All participants gave written informed consent.

Hardware, sequence & spectral analysis

All experiments used a 3T TIM Trio MR scanner (Siemens, Erlangen, Germany). The scanner's body coil was used for ^{1}H localisation. A 10 cm loop transmit-receive surface coil (Pulse Teq, Chobham, UK) tuned to the phosphorus frequency was used for spectroscopy. The ^{31}P coil was matched for each subject using an RF sweeper (Morris Instruments Inc., Ottawa, Canada). Coil loading was measured by inversion-recovery on a phenylphosphonic acid/ethanol/chromium acetylacetonate fiducial fixed at the centre of the coil, as described in reference (13), and expressed as a "reference voltage" (the RMS RF voltage giving a 1 ms 180° pulse). The ^{31}P coil was positioned above the apical myocardium of the subject. The positioning was checked using ^{1}H localiser images of the heart and coil fiducial, repositioning was carried out based on those images.

TRiST was implemented on the Siemens platform, following the description in reference (6), as follows. The vendor's 1D chemical shift imaging (CSI) sequence was modified to continuously selectively saturate a chosen frequency whilst waiting to detect an R-wave from an electrocardiogram (ECG) monitor attached to the subject. Once an R-wave was

Europe PMC Funders Author Manuscripts

detected saturation was continued for a further “trigger delay” until diastole, at which point an adiabatic half-passage (AHP) excitation pulse, 1D phase encoding gradients and free-induction-decay readout were applied. Diastole was chosen to minimise myocardial motion.

The selective saturation was provided by a train of amplitude-modulated delay alternating with nutation for tailored excitation (DANTE) pulses (6). B_1-insensitive 90° excitation was provided by frequency-cycled AHP pulses (8).

Spectra were analysed, as in reference (6), by measuring the amplitude of the phased and apodized PCr peak relative to the baseline. Raw data from TRiST scans on the 3T Achieva Philips scanner at Johns Hopkins were kindly supplied by Dr Schar and used to validate our fitting approach. k_f^{CK}, T_1' and T_1^* were calculated as described in the theory section (Eq. 1) and reference (6). The amount of direct (or spill-over) saturation of PCr by the DANTE pulse (“Q”) was calculated as the ratio of $M_{PCr}^{Ctrl}/M_{0,PCr}$. (Q = 1 in the ideal case when there is no direct saturation, but only saturation via chemical exchange from saturated γ-ATP.) Spectra from cardiac slices were selected using the transverse ^{1}H localiser and analysed on a per-slice basis.

Literature values

We surveyed the literature for values of k_f^{CK} in human myocardium and skeletal muscle (Table 3). We used the arithmetic means of the literature k_f^{CK} values and standard deviations for both tissues as a reference to validate our results.

Validation of TRiST implementation

Skeletal muscle (calf)—We validated our TRiST implementation in the calf muscle of nine healthy volunteers (8 male, 30.6±3.8 years old, 74.1±11.3 kg). The subjects were positioned feet-first-supine in the scanner with the ^{31}P loop coil under one leg. After ^{1}H localisation, the 1D-CSI grid was positioned running in the anterior-posterior direction. The protocol followed steps 1-4 in Table 2. Other parameters were: 160 mm field of view (FOV), 16 slices, 3 kHz bandwidth, 512 spectral points, and 200V AHP transmit voltage (corresponding to 800W peak power, and approximately 35 μT B_1^+ in vivo). Selective saturation of γ-ATP and control saturation were achieved using 35V DANTE pulses (corresponding to 24.5W peak power, and approximately 6 μT B_1^+ in vivo).

Myocardium in prone position—Ten healthy volunteer subjects (6 male, 29.6±4.9 years old, 70.7±18.2 kg) were scanned using the newly implemented TRiST protocol (steps 1-4, rest k_f^{CK} only) to measure myocardial k_f^{CK}. The scans were completed in the prone position as per previously published methods.

CSI acquisition parameters were as follows: 160mm FOV, 16-step matrix, 3 kHz bandwidth, 512 samples. The CSI grid was positioned perpendicular to a transverse localiser covering the heart, with the CSI delineated dimension aligned coronally (parallel to the band of skeletal muscle lying between the coil and the heart). The AHP transmit voltage was 210 V (i.e. 882W peak power), and the amplitude modulated DANTE voltage was maximised within the constraints of the specific absorption rate (SAR) for the short TR scan (typically

to ~30 V, i.e. 18W peak power). Spectra from cardiac slices were selected using the transverse ^{1}H localisers for analysis as described above. The data from the most apical slice containing only myocardium and blood (but not skeletal muscle) were also analysed separately. The coil to slice distance was < 60 mm for these slices.

Myocardium in supine position—As detailed above, as the full StreST protocol will include administering intravenous dobutamine, for which it is preferred to position the subject supine. To test whether the change of position (prone to supine) affects the initial TRiST measurement in the StreST protocol, we scanned the same ten subjects as used in the previous section (6 male, 29.6±4.9 years old, 70.7±18.2 kg) again. This time, scans were in the supine position, using the newly implemented TRiST protocol (steps 1-4, rest k_f^{CK} only). Other acquisition and analysis parameters were identical to the previous section.

Effect of intra-scan B_0 fluctuation

The potential effects of respiratory and cardiac motion induced B_0 changes on TRiST k_f^{CK} values were analysed using Bloch simulations of the full TRiST protocol. A dual-echo CINE gradient echo sequence was used to measure the range of B_0 values present in the un-shimmed apical myocardium of a single subject in different cardiac phases and respiratory states in both supine and prone positions. A sinusoidal frequency sweep with amplitude of 0, 20, 40, 60 and 80 Hz was applied to the Bloch simulation to simulate respiratory motion. The AHP pulse was simulated with three different B_1 magnitudes: 12, 23 and 35 μT, and the DANTE saturation pulse was scaled appropriately to simulate the experiment. Simulations were run with 10000 repetitions, each having a random initial cardiac and respiratory phase. Each independent step of TRiST was simulated and combined to give a measured k_f^{CK}. Simulation parameters were taken from Table 1 (Heart muscle) in Reference (14), with k_f^{CK} varied from 0.1 to 0.5 s^{-1}. SNR was calculated for PCr and γ-ATP, the simulation was scaled so the PCR SNR in step 4 was equal to 15.

Validation of MRS measured k_f^{CK} by surgical biopsy

In a cohort of 25 subjects listed for clinically indicated surgery for either severe aortic stenosis with preserved (n = 18) or impaired (n = 4) left ventricular ejection fraction (LVEF ≥ or < 55% respectively), severe primary mitral regurgitation (n = 2), or atrial myxoma (n = 1), k_f^{CK} was measured by supine TRiST and compared to CK activity measured ex-vivo from surgical LV biopsies.

All subjects pre-operatively underwent the TRiST MRS protocol in the supine position as described in the previous section. k_f^{CK} was measured for the most apical voxel identified as purely myocardium on ^{1}H localisers. Intra-operative biopsies from LV septal endocardium were obtained by the operator 10-15 minutes after cardiopulmonary bypass was established, then immediately placed into liquid nitrogen and stored at -80 °C.

For the measurement of CK activity a heaped spatula-full of frozen, crushed LV tissue was combined with CK-NAC reagent (Thermo Fisher Scientific catalogue code TR14010) and the prescribed series of reactions were monitored using a spectrophotometer to measure the

absorbance of NADH at 340nm and 37 °C over three minutes (15–17). CK activity (IU/mL) was calculated from the rate of change in absorbance of NADH, corrected for reaction volume and an assay-specific correction factor, averaged over three runs and normalised to Lowry protein (mg/mL). Results are presented as CK activity (IU/mg protein). MRS measured CK rate constant was then correlated with biopsy-measured CK activity.

Validation of the stress k_f^{CK} measurement (StreST) in healthy volunteers

The validity of the final reduced-time k_f^{CK} measurement (from steps 5 and 6 in the full StreST protocol) was tested in six healthy volunteers (male, 31±9 years, 75±8 kg). After the initial TRiST measurement (steps 1-4), the follow-on measurement (steps 5&6) was made without repositioning and with the subject still at rest (i.e. a “null stress” control condition). The PCr matched-filtered signal-to-noise ratio (SNR) of the control acquisition (step 4 in Table 2) was determined. The k_f^{Ck}, T_1', T_1^* and Q were reported.

Reproducibility of the PCr amplitude of individual scans was assessed from the 4th and 5th scans, which are acquired with identical protocols in this validation step (i.e. corresponding to rest and dobutamine-stress scans in patients). Two methods of measuring M'_{PCr} were compared: (i) by saturation-correction in TRiST; and (ii) directly from the 6th StreST step (see Table 2). The correlation and Bland-Altman statistics for these two k_f^{CK} measurements were computed.

StreST in obese subjects and age-matched controls

As many cardiac patients are obese, to allow the measurement to be validated in a real-world population, the full StreST protocol (steps 1-6), including dobutamine-induced stress during the second measurement was performed in age-matched obese and normal-weight volunteers. StreST data were acquired from an obese cohort (N=18, 5 male, 13 female, aged 49±13 years, with body-mass-index (BMI) of 35±5), and a normal-weight control cohort (N=6, 1 male, 5 female, aged 53±22 years, with BMI of 24 ± 2). TRiST alone (steps 1-4) was run in ten further normal-weight volunteers (7 male, 3 female, 40±21 years, BMI 23±3).

For stress scans, dobutamine was administered intravenously, starting at 5 μg kg^{-1} min^{-1}, and increasing the infusion rate every 3 minutes until a target heart rate of 65% maximum heart rate (i.e. 220 – age in years) was achieved; this target heart rate was then maintained at a steady state for ~18 minutes whilst the additional StreST measurements (steps 5-6) were made. Spectra from cardiac slices were selected using the transverse ^{1}H localisers for analysis as described above. The data from the most apical slice containing only myocardium and blood (but not skeletal muscle) were also analysed separately. The coil to slice distance was < 60 mm for these slices.

Results

Literature values

The results of the survey of literature k_f^{CK} are contained in Table 3. The inter-study mean ± SD k_f^{CK} values were 0.27±0.04 s^{-1} (skeletal muscle) and 0.32±0.07 s^{-1} (myocardium).

Validation of TRiST implementation

Skeletal muscle (calf)—In all subjects, seven or more slices were identified in the transverse ^{1}H localiser images as containing mainly skeletal muscle. The mean (±SD) PCr SNR in the control saturation acquisition (step 4) was 45±32. Example spectra are shown in Figure 2a.

Consistent T_1' and k_f^{CK} values were found across the 5 slices corresponding to 20 – 60 mm from the coil in all subjects. The average T_1' in these slices was 2.2±0.4 s, and k_f^{CK} was 0.25±0.03 s^{-1}. In the two slices furthest from the coil (approx. 70-80 mm), which also contained the tibia and the highest amount of subcutaneous fat, T_1' was higher and k_f^{CK} lower (Figure 2 b&e). T_1^* was less consistent across slices and between the subjects (Figure 2c).

Complete saturation (>95% saturation) of γ-ATP was observed in all subjects, in all slices except the 2 furthest from the coil; in these slices the residual γ-ATP level was 12±3% of the control saturation scan. The ratio of the control-saturation PCr peak to the no-saturation PCr peak (“Q”, a measure of direct saturation of PCr by DANTE) was >0.5 for depths from 30–80 mm (Figure 2d). In the closest slices to the coil (10 & 20 mm) Q was <0.5, i.e. substantial direct saturation occurred.

Results from this subsection and others in “results” are summarised in Supporting Table 1.

Myocardium in prone position—From the ten healthy volunteers scanned in the prone position, 29 slices were identified as corresponding to myocardium in the transverse ^{1}H localisers and had sufficient SNR for analysis (PCr SNR > 10 in the control scan).

The all-slice mean ± SD k_f^{CK} was 0.29±0.09 s^{-1}. Analysing only the most anterior purely myocardial slice in each subject (10 slices) gave mean k_f^{CK} of 0.32±0.15 s^{-1}.

The all-slice mean T_1' was 2.7 ± 1.0 s and T_1* was 4.7±1.6 s. The mean (±SD) PCr SNR was 18 ± 8. Analysing only the most anterior purely myocardial slice in each subject gave SNR = 19 ± 5, T_1' = 2.9 ± 0.6 s, and T_1* = 5.2±0.8 s.

Myocardium in supine position—The same ten healthy volunteers were also scanned in the supine position. In this dataset, 30 slices were identified as corresponding to myocardium in the transverse ^{1}H localisers and had sufficient SNR for analysis.

The all-slice mean ± SD k_f^{CK} was 0.15±0.10 s^{-1}. Analysing only the most anterior purely myocardial slice in each subject gave a mean k_f^{CK} of 0.24±0.12 s^{-1}.

The all-slice T_1' was 2.5 ± 1.1 s, and T_1* was 4.4±1.9 s. The mean (±SD) PCr SNR was 16 ± 9. Analysing only the most anterior purely myocardial slice in each subject gave SNR = 17 ± 6, T_1' = 2.3 ± 0.5 s, and T_1* = 4.6±1.0 s.

Effect of intra-scan B_0 fluctuation

The single subject measurement of B_0 established that the mean range of γB_0 experienced in the apical myocardium due to cardiac motion in a ^{31}P experiment is 34.3 Hz (supine) and 34.6 Hz (prone), and due to respiratory motion is 66.7 Hz (supine) and 36.1 Hz (prone). (Supporting Figure 1 & 2). As the range of B_0 variation was increased in the simulations the amount of time during the DANTE saturation pulse when $M_{z,\gamma\text{-ATP}} = 0$ decreased (i.e. γ-ATP saturation was not achieved at all times), even though the SNR of the residual γ-ATP peak in TRiST steps 2&3 remained very low: SNR < 2.5 (Figure 3 a&b). With increasing B_0 fluctuation amplitude and decreasing γ-ATP saturation, the measured k_f^{CK} also decreased (Figure 3c). At the level of the estimated B_0 variation due to respiration in our study, the measured k_f^{CK} was simulated to be 0.61 times the true k_f^{CK} in a supine position and 0.85 times the true k_f^{CK} in the prone position. The linearity of the ratio of measured k_f^{CK} / true k_f^{CK} decreases with increasing B_0 variation (Figure 3d).

Validation of MRS measured k_f^{CK} by surgical biopsy

From the twenty-five subjects listed for clinically indicated surgery mean (±SD) k_f^{CK} was 0.21±0.10 s^{-1} and mean (±SD) biopsy-measured CK activity was 3.96±1.70 IU mg^{-1} protein. The Pearson's Linear Correlation Coefficient (Pearson's R) was 0.43 with a statistically significant correlation (p = 0.03).

Validation of the stress k_f^{CK} measurement (StreST) in healthy volunteers

All the per-subject and mean k_f^{CK} values from the myocardial and skeletal muscle voxels of the six healthy volunteer rest-rest ("null stress" control) StreST scans are plotted in Figure 4. In these scans 36 slices were identified as corresponding to myocardium in the transverse ^1H localisers and had sufficient SNR for analysis (PCr SNR > 10 in the control scan). The all-slice mean (±SD) PCr SNR was 16 ± 9, T_1' was 2.9 ± 1.0 s, and T_1* was 4.8±1.8 s. The all-slice mean k_f^{CK} of the first measurement (TRiST) was 0.14±0.08 s^{-1} and the all-slice mean of the second measurement (dobutamine not administered for this validation experiment) was 0.22±0.14 s^{-1}. A per-slice comparison of these k_f^{CK} measurements yielded a correlation of 0.51 (Figure 5a). Bland-Altman (Figure 5b) analysis yielded a bias of -0.08 s^{-1} with 95% confidence intervals (CIs) of +0.16 s^{-1} and −0.31 s^{-1}. A paired Student's t-test showed statistical significance between the two measurements (p = 0.0006).

Analysing only the most anterior purely myocardial slice in each subject (6 slices) gave SNR = 15 ± 5, PCr T_1' = 3.0 ± 0.6 s, PCr T_1* = 5.7±0.9 s, k_f^{CK} (first) = 0.18±0.08 s^{-1}, k_f^{CK} (second) = 0.18±0.05 s^{-1}, and a per-slice correlation of 0.62. The mean coil-to-voxel distance for these slices was 53±7 mm. Bland-Altman (Figure 5b) analysis yielded a bias of -0.04 s^{-1} with 95% CIs of +0.04 s^{-1} and −0.12 s^{-1}. A paired Student's t-test showed no statistical significance between the two measurements (p = 0.11).

Further reproducibility measurements are presented in the supporting information. The comparison of the PCr amplitudes of the 4th and 5th steps yielded a correlation of 0.99 (Supporting Figure 3a&b). The comparison of the two methods of calculating M_0' yielded a correlation of 0.96 (Supporting Figure 3c&d).

Europe PMC Funders Author Manuscripts

The coil reference voltage, measuring the degree of coil loading, varied by <10 % for all six subjects, and was within 25% of the values measured in the skeletal muscle validation.

StreST in obese subjects and age-matched controls

In both obese and normal-weight volunteers (34 total) the average k_f^{CK} in all myocardial slices (with PCr SNR > 10) was 0.12±0.08 s^{-1}. The average PCr SNR was 14±9 across the 209 slices analysed.

Analysing only the most anterior myocardial slice of each subject (34 slices), k_f^{CK} was 0.16±0.08 s^{-1} (Figure 6a). The average PCr SNR was 15±6.

In the subjects that underwent both rest & stress measurements the mean k_f^{CK} at rest was 0.16±0.07 s^{-1} (obese) and 0.15±0.09 s^{-1} (normal weight). Under stress the values were 0.17±0.11 s^{-1} (obese) and 0.17±0.15 s^{-1} (normal weight). This data is shown in Figure 6b.

The T_1* of the two cohorts was 5.69±1.43 s for obese and 4.67±1.92 s for normal weight subjects (Figure 6c); this difference is statistically significantly (Student's t-test, p = 0.02).

Discussion

We have implemented a new StreST protocol for measuring human CK rate constants in the human heart during dobutamine-induced stress. In so doing, we have also implemented the published TRiST protocol measuring k_f^{CK} at rest for the first time on a Siemens scanner, and using a commercially available coil. We have tested StreST (and hence also TRiST) in calf and cardiac muscle and applied it in the hearts of normal volunteers and obese subjects. We have demonstrated a correlation between our MRS measured value of k_f^{CK} and CK activity in human LV biopsies.

Measurements in calf muscle show that our implementation of TRiST measures k_f^{CK} in line with literature values up to 70 mm from coil. The coil loading changed by up to 25% between skeletal muscle and the thorax. Therefore, we expected accurate myocardial measurement in cardiac slices ≤70 mm from the coil, i.e. we expected that k_f^{CK} in apical cardiac slices could be measured robustly. This is corroborated by a Monte Carlo propagation of error analysis (Supporting Figure 4) which suggests the precision and accuracy of the technique is acceptable for PCr SNR > 10. Only apical myocardial slices achieve this SNR level consistently in all subjects. The working depth of the TRiST protocol could be improved by a different choice of coil: e.g. a different design of transmit coil (e.g. a larger loop or two loops in quadrature) would ensure effective saturation and excitation at greater depths. A receive array might also be used for signal reception to improve SNR, although this might come at the expense of greatly increased signal contamination by non-myocardial tissue because spatial localisation in TRiST is reliant on a restricted sensitivity profile of the coil in two dimensions.

Myocardial k_f^{CK} measured in the prone position further validated the new implementation of TRiST with all cardiac slices in ten subjects giving 0.29±0.09 s^{-1} and k_f^{CK} from only the most apical voxel for each subject giving a mean of 0.32±0.15 s^{-1}, although the standard deviation of this measurement is double that reported in the literature (Table 3). In the supine

position, the measured k_f^{CK} throughout this study is much lower than the paired prone estimate, the literature estimate of 0.32 s^{-1}, and our own 7T k_f^{CK} estimate (0.35±0.05) (9). It is therefore likely that the absolute value of k_f^{CK} measured in a supine position is an underestimate. However, simulations of the effect of B_0 variation during respiratory and cardiac cycles and correlation with biopsy measured CK activity in 25 patients indicate that despite the low absolute value of supine MRS measured k_f^{CK}, trends in our measured k_f^{CK} values are still meaningful – i.e. increases or decreases in measured k_f^{CK} correspond to real increases or decreases.

We invested considerable effort in studying the possible causes of the lower supine TRiST k_f^{CK} measurements. A thorough validation of the sequence timings was performed in the vendor simulation environment and by capturing the live waveforms of the triggered sequence using a digital oscilloscope on the scanner. Data shared from Johns Hopkins were used to validate our analysis process, which performed comparably to the Johns Hopkins analysis. Bloch simulations of the TRiST method indicated that if constant steady-state saturation of γ-ATP is not maintained completely throughout the mixing time, the measured k_f^{CK} will underestimate the true k_f^{CK} by a predictable scaling that is approximately linear for modest B_0 fluctuation amplitudes (Supporting Figure 5). Note that this effect can occur even when the γ-ATP peak is well suppressed in the observed saturated spectra. It is proposed that this is produced by B_0 shifts, due to respiration or cardiac motion, intermittently shifting the γ-ATP resonance away from the target selective saturation frequency. We have shown that the range of B_0 experienced in the myocardium is raised in this experiment when the subject is supine rather than prone (approx. 60 Hz range versus 30 Hz). The choice of supine scanning was necessitated in this study for subject safety during pharmacological stress and will be required in our institute for further studies using StreST in patients with established cardiac diseases. Scanning supine also helps coil placement and matching.

The effect of B_0 shifts due to respiration was found, by simulation, to decrease the measured k_f^{CK} by approximately 1.6 times for supine scans. This factor was found to be constant for all values of k_f^{CK} as long as the B_0 shifts did not exceed a range of 80 Hz. Above this level the effect is non-linear, decreasing the sensitivity of TRiST to changes in k_f^{CK}. Our simulations also suggest that even in the prone position the true value of k_f^{CK} is likely to be underestimated by the TRiST method. At the measured amplitude of B_0 fluctuation the correction remains mostly linear and so relative changes in k_f^{CK} are preserved for both prone and supine scanning.

StreST reduces the time of the consecutive measurement from 40 min to 20 min by assuming that the subject's T_1* is constant, which makes it feasible to measure k_f^{CK} during dobutamine infusion at 3T. Previously, Weiss et al. used an adaptation of the "FAST" protocol to measure k_f^{CK} during stress in 13 minutes at 1.5 T (1). The validation of StreST applied without dobutamine showed that the method is able to reliably measure the same k_f^{CK} in a reduced duration in the most apical, high SNR voxels. It is therefore likely that the assumption of static between-scan T_1* is reasonable. In voxels with low SNR or experiencing high direct saturation (low Q, e.g. skeletal muscle) the reduced duration measurement does not match the full TRiST measurement and introduces high variance.

The average PCr T_1* calculated, as per Eqn. 2, was different for the two cohorts: normal-weight and obese (p=0.02). This suggests that to accurately measure stress k_f^{CK}, T_1* must either be determined per-subject, as in StreST, or per-cohort in a pilot study designed to measure T_1*. We do not recommend assuming a single PCr T_1* for all human subjects.

Like TRiST, StreST has diagnostic potential for non-invasively assessing the CK system and by extension a subject's contractile reserve (18). Sensitivity to contractile reserve would be valuable in patients who are not able to undergo conventional stress testing e.g. severe valvular heart disease. The CK system is also a major mechanism for controlling cytosolic [ADP]. A raised cytosolic [ADP] at stress contributes to increased left ventricular end-diastolic pressure and diastolic dysfunction (19). A raised left ventricular end-diastolic pressure is characteristic of heart failure with preserved ejection fraction, which comprises approximately half of all clinically presenting heart failure cases.

Cardiac positron emission tomography (PET) can also measure myocardial metabolic reaction kinetics through the uptake of tracers (20). It is able to confirm viability in suspected hibernating myocardium using glucose tracers (21). PET is able to detect uptake in ingressing inflammatory cells and has emerging roles in detection of prosthetic valve endocarditis (22) and inflammatory atherosclerotic coronary and carotid plaques (23,24). However, the onward metabolism of the tracer after uptake cannot be assessed and it is not possible to distinguish which cell type is responsible using PET alone. The MRS technique presented here is specific to CK expressing cells, i.e. cardiomyocytes. Cardiac MR(S) and PET measure similar information with differing trade-offs in temporal and spatial resolution. The use of both in tandem could offer complementary information (21).

StreST was demonstrated in a control cohort, as well as an obese cohort. The TRiST component of the protocol was run successfully on 34 out of 35 initial subjects. The full StreST protocol was completed by 17 out of 24 subjects, with five subjects electing not to complete due to discomfort and two scans stopped after exceeding the local limit on maximum scan duration. The mean ± SD time of a complete StreST protocol was 103±7 minutes, Steps 1-6 of StreST take 64 minutes in total. The TRiST and StreST techniques are being applied in ongoing studies, building on the initial cohort scans in this work.

Conclusion

In this work, we introduced an extended StreST protocol that enables measurement of k_f^{CK} during a 20-minute dobutamine infusion at 3T. We also independently implemented the TRiST protocol on a Siemens 3T scanner using commercially-available hardware. We compare TRiST measured in the prone and supine position and provide a non-MR validation of MR measured k_f^{CK}. We show by simulations that respiratory-induced motion can lead to incomplete γ-ATP saturation during the saturation-transfer phase of the TRiST sequence even in the case where the γ-ATP peak is absent from the saturated spectra. Linear correction can compensate for these effects for light to moderate B_0-field fluctuation amplitudes.

Acknowledgements

We thank Michael Schar for providing test data to validate our post-processing routines, and Paul Bottomley for discussion of the potential factors that may reduce measured k_f^{CK}.

Funded by: a Sir Henry Dale Fellowship from the Wellcome Trust and the Royal Society [098436/Z/12/B] to CTR, the BHF Centre of Research Excellence (OJR), a BHF clinical research training fellowship [FS/15/80/31803] to MAP, a BHF fellowship [FS/14/54/30946] to JJR, an NIHR OBRC fellowship to BR, a BHF programme grant [RG/13/8/30266] to CAL and SN, and a DPhil studentship from the Medical Research Council to WTC. We acknowledge support from the Oxford NIHR Biomedical Research Centre.

Abbreviations

AHP	adiabatic half-passage (pulse)
ATP	adenosine triphosphate
BMI	body-mass-index
CK	creatine kinase
CSI	chemical shift imaging
DANTE	delay alternating with nutation for tailored excitation
ECG	electrocardiogram
FAST	four-angle saturation transfer
k_f^{CK}	pseudo first-order forward rate
LV	left ventricular
PCr	phosphocreatine
StreST	stress saturation-transfer
TRiST	triple repetition time saturation transfer
TwiST	Two repetition time saturation transfer

References

1. Weiss RG, Gerstenblith G, Bottomley PA. ATP flux through creatine kinase in the normal, stressed, and failing human heart. P Natl Acad Sci USA. 2005; 102(3):808–813.
2. Mozaffarian D, Benjamin EJ, Go AS, et al. Heart disease and stroke statistics--2015 update: a report from the American Heart Association. Circulation. 2015; 131(4):e29–322. [PubMed: 25520374]
3. Townsend, N, Williams, J, Bhatnagar, P, Wickramasinghe, K, Rayner, M. Cardiovascular disease statistics, 2014. London: British Heart Foundation; 2014.
4. Bottomley PA, Ouwerkerk R, Lee RF, Weiss RG. Four-angle saturation transfer (FAST) method for measuring creatine kinase reaction rates in vivo. Magn Reson Med. 2002; 47(5):850–863. [PubMed: 11979563]
5. Rider OJ, Francis JM, Ali MK, et al. Effects of catecholamine stress on diastolic function and myocardial energetics in obesity. Circulation. 2012; 125(12):1511–1519. [PubMed: 22368152]

Europe PMC Funders Author Manuscripts

6. Schar M, El-Sharkawy AMM, Weiss RG, Bottomley PA. Triple Repetition Time Saturation Transfer (TRiST) (31)P Spectroscopy for Measuring Human Creatine Kinase Reaction Kinetics. Magnetic Resonance in Medicine. 2010; 63(6):1493–1501. [PubMed: 20512852]
7. Schar M, Gabr RE, El-Sharkawy AM, Steinberg A, Bottomley PA, Weiss RG. Two repetition time saturation transfer (TwiST) with spill-over correction to measure creatine kinase reaction rates in human hearts. J Cardiovasc Magn R. 2015; 17
8. El-Sharkawy AM, Schar M, Ouwerkerk R, Weiss RG, Bottomley PA. Quantitative Cardiac P-31 Spectroscopy at 3 Tesla Using Adiabatic Pulses. Magnetic Resonance in Medicine. 2009; 61(4): 785–795. [PubMed: 19195018]
9. Clarke WT, Robson MD, Neubauer S, Rodgers CT. Creatine kinase rate constant in the human heart measured with 3D-localization at 7 tesla. Magn Reson Med. 2017; 78(1):20–32. [PubMed: 27579566]
10. Becher H, Chambers J, Fox K, et al. BSE procedure guidelines for the clinical application of stress echocardiography, recommendations for performance and interpretation of stress echocardiography: a report of the British Society of Echocardiography Policy Committee. Heart. 2004; 90(Suppl 6):vi23–30. [PubMed: 15564422]
11. Spencer RG, Fishbein KW. Measurement of spin-lattice relaxation times and concentrations in systems with chemical exchange using the one-pulse sequence: breakdown of the Ernst model for partial saturation in nuclear magnetic resonance spectroscopy. J Magn Reson. 2000; 142(1):120–135. [PubMed: 10617442]
12. Geleijnse ML, Krenning BJ, Nemes A, et al. Incidence, pathophysiology, and treatment of complications during dobutamine-atropine stress echocardiography. Circulation. 2010; 121(15): 1756–1767. [PubMed: 20404267]
13. Rodgers CT, Clarke WT, Snyder C, Vaughan JT, Neubauer S, Robson MD. Human cardiac 31P magnetic resonance spectroscopy at 7 Tesla. Magn Reson Med. 2014; 72(2):304–315. [PubMed: 24006267]
14. Ouwerkerk R, Bottomley PA. On neglecting chemical exchange effects when correcting in vivo (31)P MRS data for partial saturation. J Magn Reson. 2001; 148(2):425–435. [PubMed: 11237649]
15. Oliver IT. A spectrophotometric method for the determination of creatine phosphokinase and myokinase. Biochem J. 1955; 61(1):116–122. [PubMed: 13260184]
16. Rosalki SB. An improved procedure for serum creatine phosphokinase determination. J Lab Clin Med. 1967; 69(4):696–705. [PubMed: 4381359]
17. Szasz G, Waldenstrom J, Gruber W. Creatine-Kinase in Serum .6. Inhibition by Endogenous Polyvalent Cations, and Effect of Chelators on the Activity and Stability of Some Assay Components. Clin Chem. 1979; 25(3):446–452. [PubMed: 45380]
18. Tian R, Nascimben L, Kaddurah-Daouk R, Ingwall JS. Depletion of energy reserve via the creatine kinase reaction during the evolution of heart failure in cardiomyopathic hamsters. J Mol Cell Cardiol. 1996; 28(4):755–765. [PubMed: 8732503]
19. Tian R, Nascimben L, Ingwall JS, Lorell BH. Failure to maintain a low ADP concentration impairs diastolic function in hypertrophied rat hearts. Circulation. 1997; 96(4):1313–1319. [PubMed: 9286964]
20. Sarikaya I. Cardiac applications of PET. Nucl Med Commun. 2015; 36(10):971–985. [PubMed: 26035516]
21. Kunze KP, Dirschinger RJ, Kossmann H, et al. Quantitative cardiovascular magnetic resonance: extracellular volume, native T1 and 18F-FDG PET/CMR imaging in patients after revascularized myocardial infarction and association with markers of myocardial damage and systemic inflammation. J Cardiovasc Magn Reson. 2018; 20(1):33. [PubMed: 29792210]
22. Habib G, Lancellotti P, Antunes MJ, et al. 2015 ESC Guidelines for the management of infective endocarditis: The Task Force for the Management of Infective Endocarditis of the European Society of Cardiology (ESC). Endorsed by: European Association for Cardio-Thoracic Surgery (EACTS), the European Association of Nuclear Medicine (EANM). Eur Heart J. 2015; 36(44): 3075–3128. [PubMed: 26320109]

23. Moss AJ, Adamson PD, Newby DE, Dweck MR. Positron emission tomography imaging of coronary atherosclerosis. Future Cardiol. 2016; 12(4):483–496. [PubMed: 27322032]
24. Salata BM, Singh P. Role of Cardiac PET in Clinical Practice. Curr Treat Options Cardiovasc Med. 2017; 19(12):93. [PubMed: 29119262]
25. Smith CS, Bottomley PA, Schulman SP, Gerstenblith G, Weiss RG. Altered creatine kinase adenosine triphosphate kinetics in failing hypertrophied human myocardium. Circulation. 2006; 114(11):1151–1158. [PubMed: 16952984]
26. Bottomley PA, Wu KC, Gerstenblith G, Schulman SP, Steinberg A, Weiss RG. Reduced Myocardial Creatine Kinase Flux in Human Myocardial Infarction An In Vivo Phosphorus Magnetic Resonance Spectroscopy Study. Circulation. 2009; 119(14):1918–1924. [PubMed: 19332463]
27. Bashir A, Gropler R. Reproducibility of creatine kinase reaction kinetics in human heart: a 31P time-dependent saturation transfer spectroscopy study. NMR in Biomedicine. 2014; 27(6):663–671. [PubMed: 24706347]
28. Valkovic L, Chmelik M, Kukurova IJ, et al. Time-resolved phosphorous magnetization transfer of the human calf muscle at 3 T and 7 T: A feasibility study. Eur J Radiol. 2013; 82(5):745–751. [PubMed: 22154589]
29. Parasoglou P, Xia D, Chang G, Convit A, Regatte RR. Three-dimensional mapping of the creatine kinase enzyme reaction rate in muscles of the lower leg. Nmr in Biomedicine. 2013; 26(9):1142–1151. [PubMed: 23436474]
30. Parasoglou P, Xia D, Chang G, Regatte RR. Three-dimensional Saturation Transfer P-31-MRI in Muscles of the Lower Leg at 3.0 T. Sci Rep-Uk. 2014; 4
31. Valkovic L, Bogner W, Gajdosik M, et al. One-Dimensional Image-Selected In Vivo Spectroscopy Localized Phosphorus Saturation Transfer at 7T. Magnetic Resonance in Medicine. 2014; 72(6): 1509–1515. [PubMed: 24470429]
32. Buehler T, Kreis R, Boesch C. Comparison of 31P saturation and inversion magnetization transfer in human liver and skeletal muscle using a clinical MR system and surface coils. Nmr in Biomedicine. 2015; 28(2):188–199. [PubMed: 25483778]
33. Ren JM, Sherry AD, Malloy CR. P-31-MRS of healthy human brain: ATP synthesis, metabolite concentrations, pH, and T-1 relaxation times. Nmr in Biomedicine. 2015; 28(11):1455–1462. [PubMed: 26404723]

Europe PMC Funders Author Manuscripts

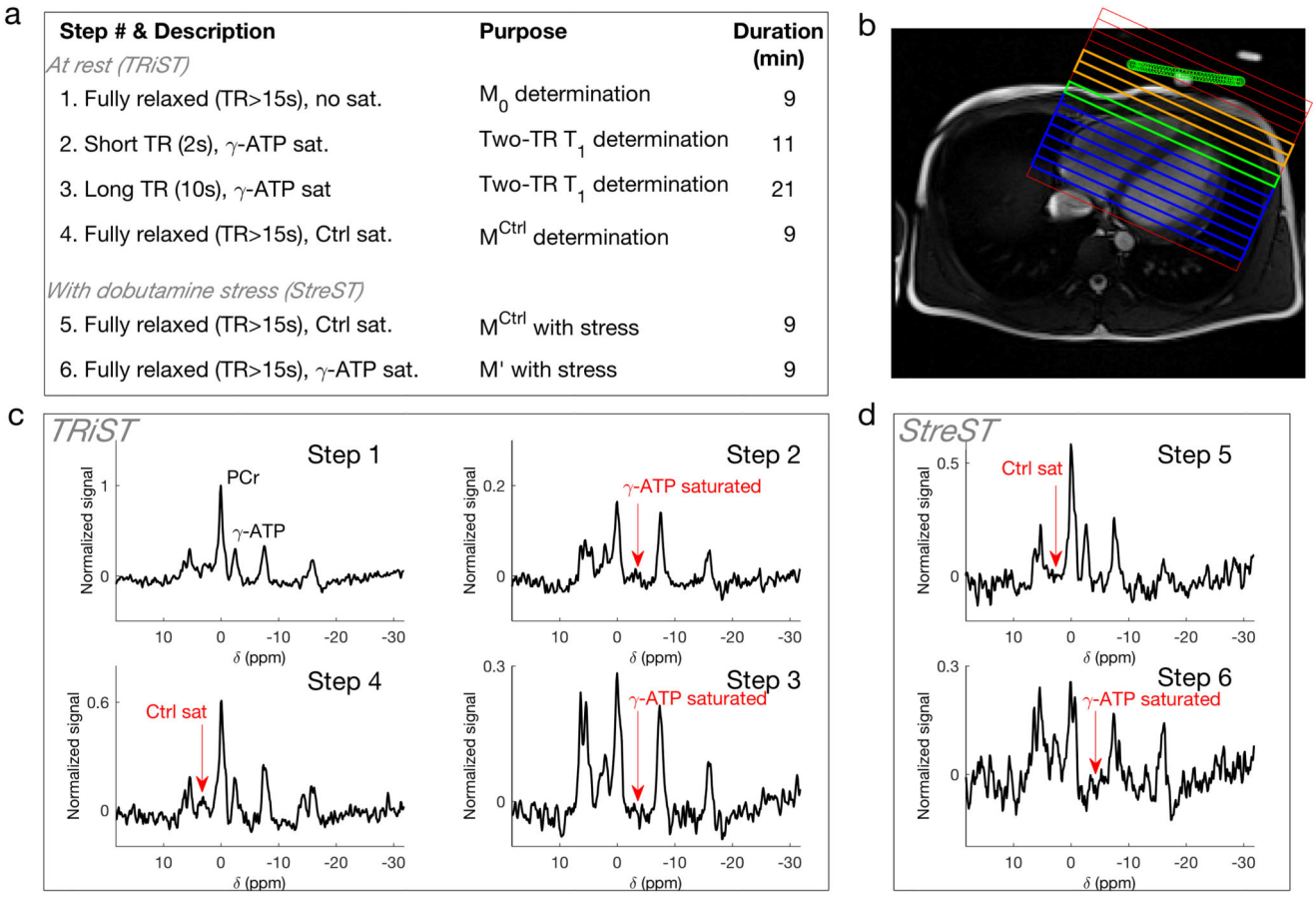

Figure 1.

a Six-step StreST protocol (including TRiST as steps 1-4). **b** 1H localiser with 1D CSI grid overlaid. The coil position is marked in green. Orange = Skeletal muscle, Blue = myocardium, green = Most anterior myocardial slice (coil slice distance < 60 mm). **c** Spectra acquired from the 4 steps of TRiST on a healthy, normal-weight subject. **d** Spectra acquired during dobutamine stress as part of the extension StreST measurement. In **c**&**d** signal is normalised to the PCr peak value in step 1.

Europe PMC Funders Author Manuscripts

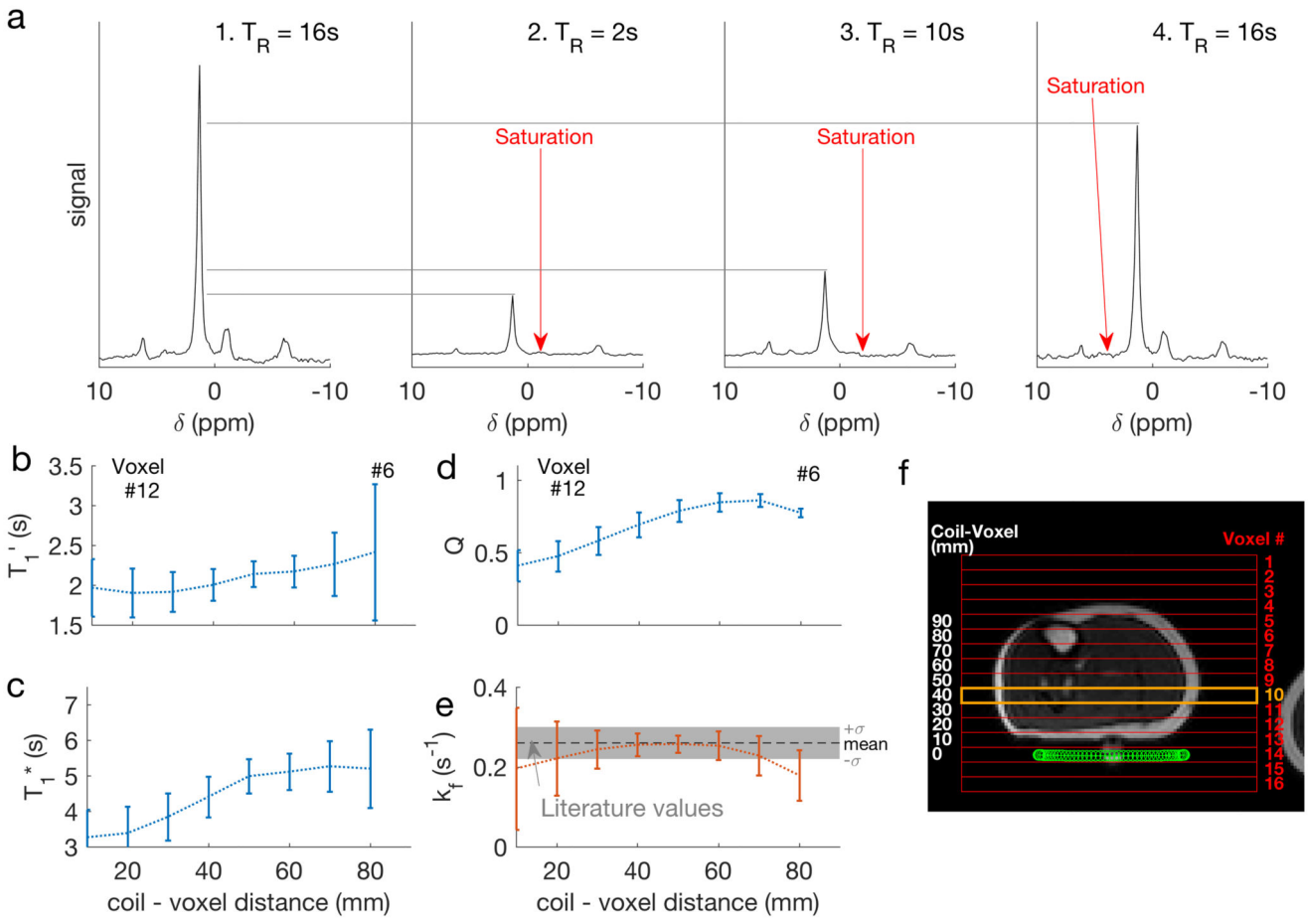

Figure 2.

a Spectra from the four constituent scans of TRiST, showing the site of selective saturation, taken from a single slice in one subject (number 10, marked in orange in **f**). **b** Saturation-affected T_1 (T_1') for each subject in each slice, plotted as a function of distance from the coil. Error bars indicate (mean ± SD). **c** shows the intrinsic T_1 (T_1*), **d** the amount of direct PCr saturation (Q), **e** the k_f^{CK}, and **f** shows a localiser with a CSI grid overlaid (red), the slice plotted (orange), and the coil position (green).

Europe PMC Funders Author Manuscripts

Europe PMC Funders Author Manuscripts

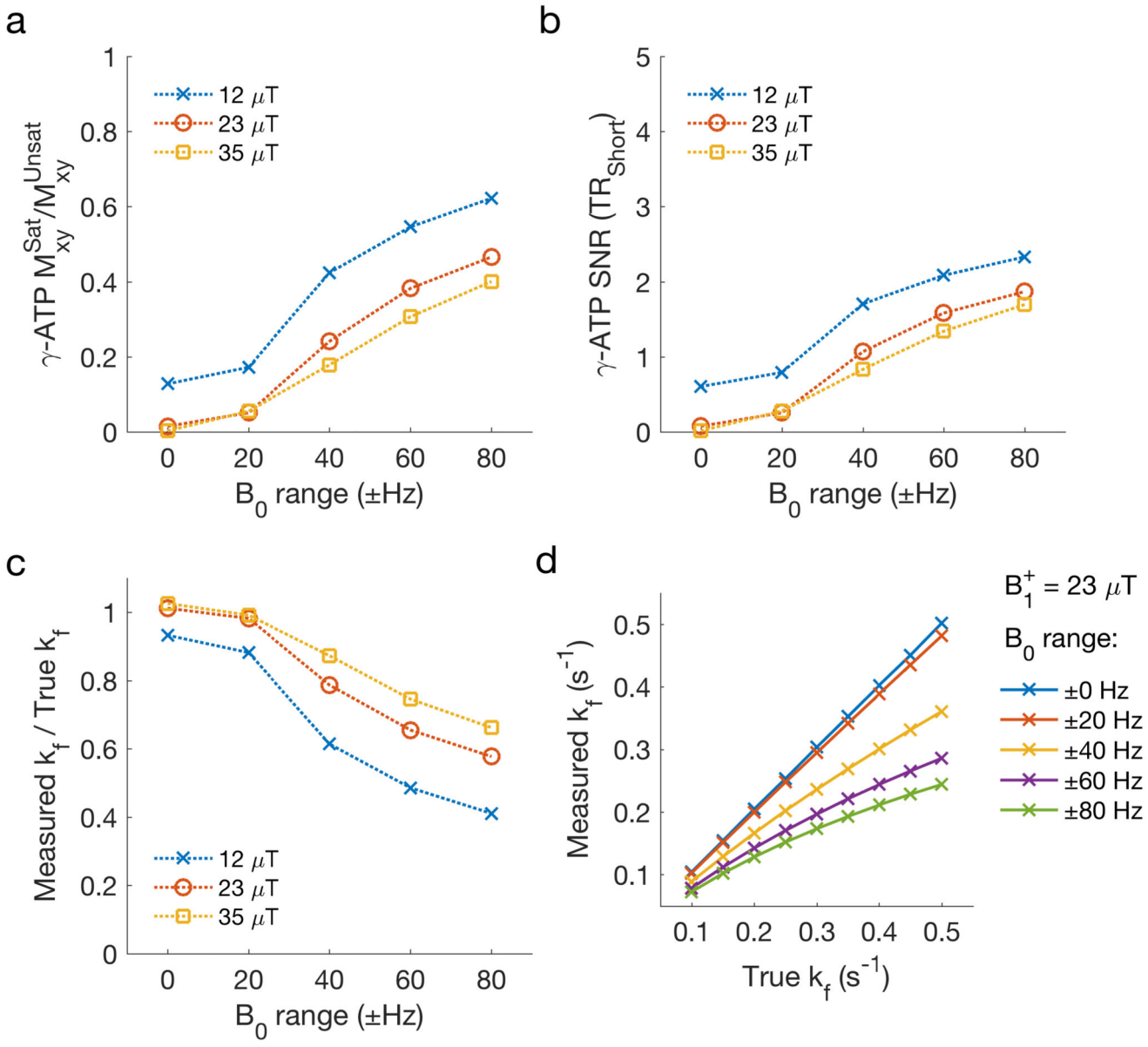

Figure 3.

Simulated effect of respiration on the measurement of k_f^{CK}. **a** The ratio of γ-ATP transverse magnetisation in the presence of steady-state saturation (with respiration induced B_0 variation) versus the same sequence with no steady-state saturation. **b** The residual γ-ATP peak SNR. **c** The ratio of measured k_f^{CK} to true (simulation) k_f^{CK}. True $k_f^{CK} = 0.30\ s^{-1}$. **d** Measured k_f^{CK} in the presence of respiration induced B_0 variation at different values of true k_f^{CK}.

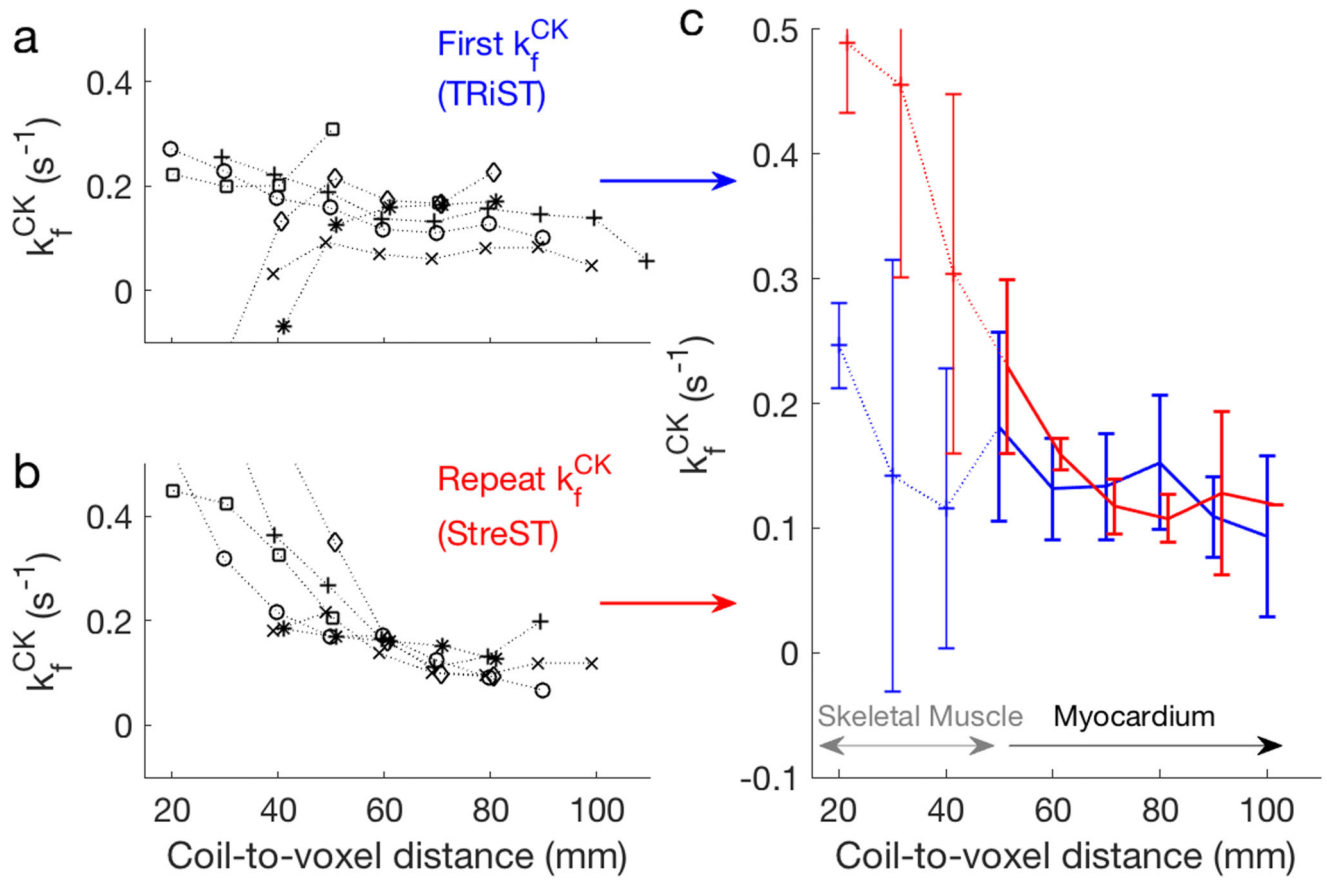

Figure 4.

a TRiST and **b** StreST measured k_f^{CK} in the chest of six normal volunteers. Results are plotted as a function of coil-slice distance. StreST was performed without dobutamine stress for this validation study. Different markers denote different subjects. In **c** the inter-subject mean and standard deviation k_f^{CK} is shown for TRiST (blue: also 1st measurement of StreST) and the second measurement of StreST (red).

Europe PMC Funders Author Manuscripts

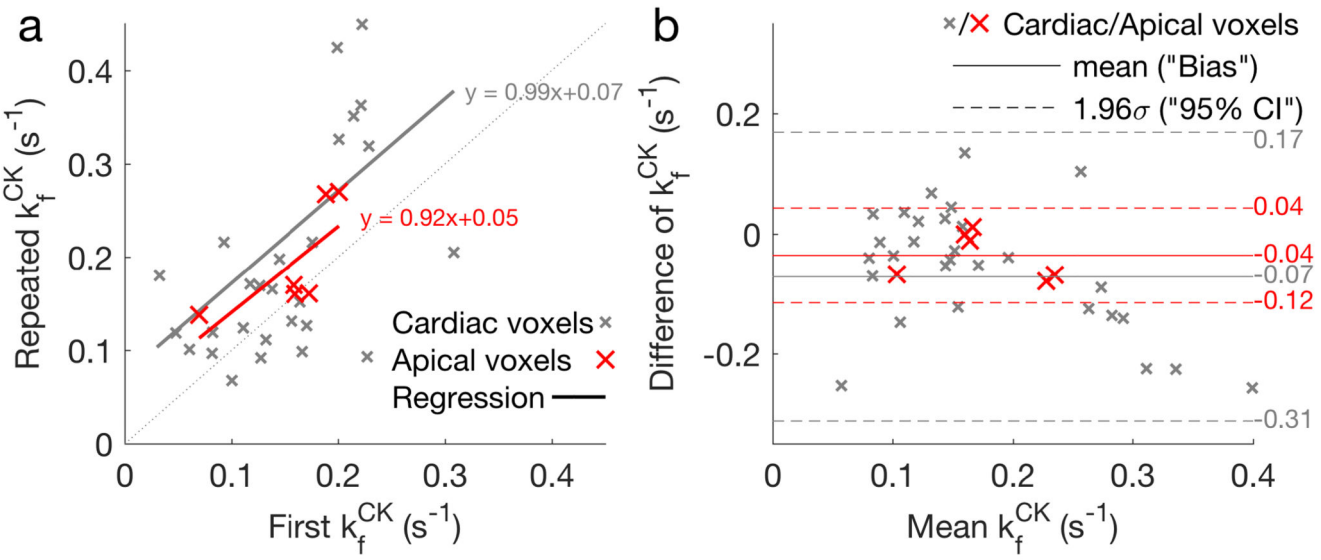

Figure 5.

a Per-slice correlation plot of the two k_f^{CK} measurements in StreST (1st measurement equivalent to TRiST). All myocardial slices are shown, with the most apical cardiac slice for each subject shown in red. Results of linear regressions are also shown. **b** Bland-Altman comparison of the two k_f^{CK} measurements. The bias and 95% confidence intervals for each set of slices (all cardiac & apical) are marked.

Europe PMC Funders Author Manuscripts

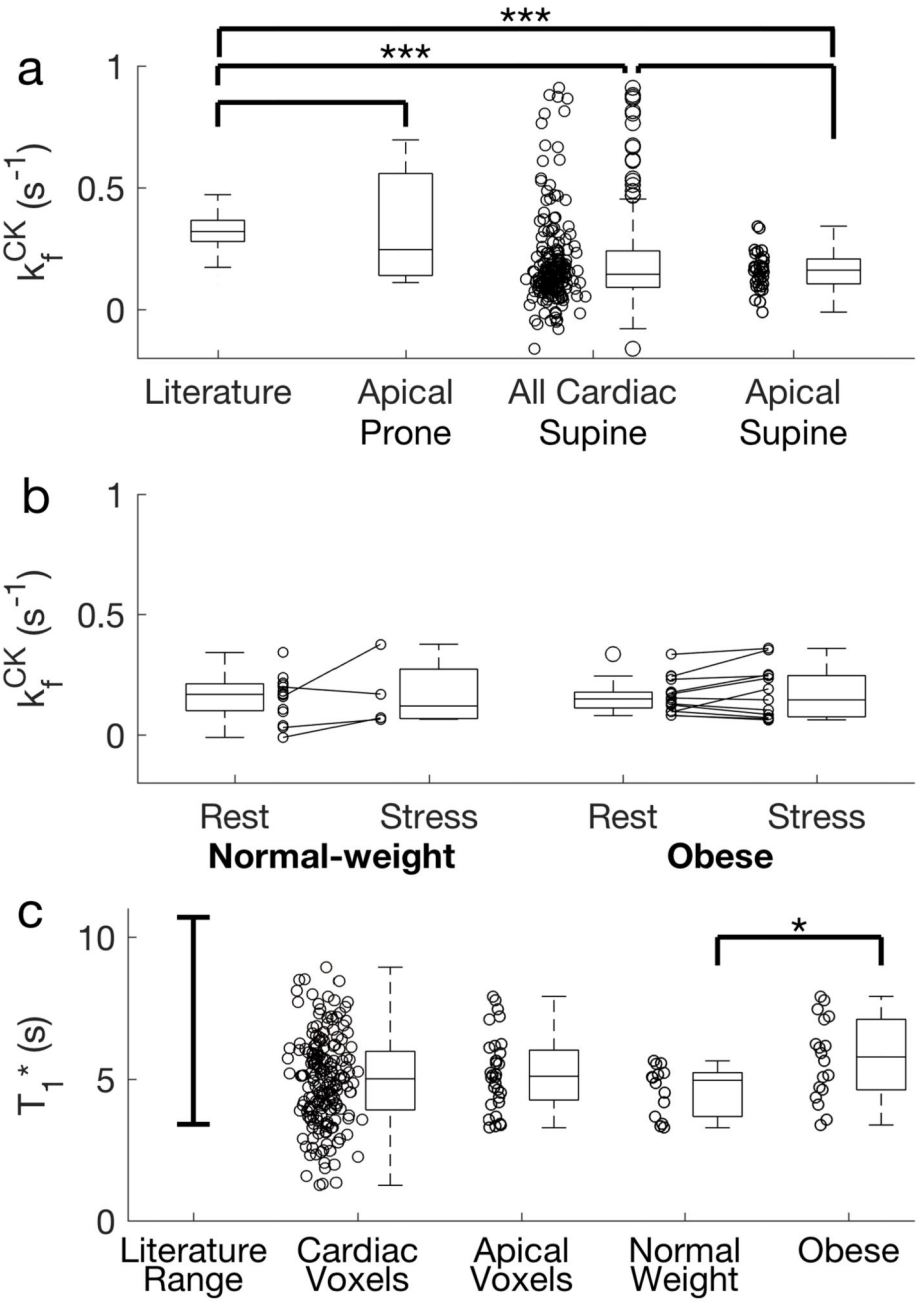

Figure 6.

a The measured k_f^{CK} in all subjects undergoing the 4 scan TRiST measurement. Shown are the results from the prone validation, and all myocardial slices and anterior myocardial slices from supine scans. **b** Rest and stress measurements from the selected slices of 34 normal-weight and obese volunteers. Negative values of k_f^{CK} are shown in this plot. Whilst negative k_f^{CK} values are not physically meaningful, they arise from noise entering into Equation 1. **c** Reported literature range of intrinsic T_1 (T_1*)(7) compared to that measured in this study,

for all cardiac slices, the most apical cardiac slices, and the apical cardiac slices from normal weight and obese subjects.

Europe PMC Funders Author Manuscripts

Europe PMC Funders Author Manuscripts

Table 1

Meaning of equation variables.

Symbol	Meaning
$M_{0,\mathrm{PCr}}$	Equilibrium longitudinal magnetisation of PCr
$M_{\mathrm{PCr}}^{\mathrm{Ctrl}}$	Measured steady-state longitudinal PCr magnetisation, with mirrored control saturation applied.
$T_{\mathrm{R}}^{\mathrm{Short/Long}}$	Short and long T_R, where both $T_{\mathrm{R}}^{\mathrm{Short/Long}} < 5T_1$.
M'_{PCr}	Longitudinal PCr magnetisation, with on-resonance saturation of γ-ATP applied. $T_R \approx 5T_1$
$M'_{\mathrm{PCr}}(T_{\mathrm{R}}^{\mathrm{Short}}/T_{\mathrm{R}}^{\mathrm{Long}})$	Measured steady-state longitudinal PCr magnetisation, with on-resonance saturation of γ-ATP applied.
T'_1	Measured T_1 in the presence of on-resonance saturation of γ-ATP applied.
T_1^*	Intrinsic T_1, i.e. without the effect of exchange.

Europe PMC Funders Author Manuscripts

Table 2

Acquisition parameters for the StreST protocol. The first four steps are those of TRiST(6). […] are parameters required for spill-over correction of k_f^{CK}.

#	θ	T_R (s)	Saturation target	Scan averages	Duration (min)	Measured parameters		
1	90°	≥15	-	2	9	$M_{0,\mathrm{PCr}}$, $M_{0,\gamma\text{-ATP}}$	TRiST	StreST
2	90°	$2\left(T_R^{\mathrm{Short}}\right)$	γ-ATP	18	11	$M'_{\mathrm{PCr}}(T_R^{\mathrm{Short}}), \left[M'_{\gamma\text{-ATP}}(T_R^{\mathrm{Short}})\right]$		
3	90°	$10\,(T_R^{\mathrm{Long}})$	γ-ATP	8	21	$M'_{\mathrm{PCr}}(T_R^{\mathrm{Long}}), \left[M'_{\gamma\text{-ATP}}(T_R^{\mathrm{Long}})\right]$		
4	90°	≥15	Control	2	9	$M_{\mathrm{PCr}}^{\mathrm{Ctrl}}, M_{\gamma-\mathrm{ATP}}^{\mathrm{Ctrl}}$		
5	90°	≥15	Control	2	9	$M_{\mathrm{PCr}}^{\mathrm{Ctrl}}, M_{\gamma-\mathrm{ATP}}^{\mathrm{Ctrl}}$		
6	90°	≥15	γ-ATP	2	9	$M'_{\mathrm{PCr}}, \left[M'_{\gamma-\mathrm{ATP}}\right]$		

Europe PMC Funders Author Manuscripts

Table 3

Literature values for human in vivo k_f^{CK} in normal volunteers at rest.

Reference	Method[1]	Localisation[2]	Field (T)	N	Study mean ± SD or range (s^{-1})
Myocardium					
(1)	FAST	1D-CSI	1.5	16	0.32±0.07
(25)	FAST	1D-CSI	1.5	14	0.32±0.06
(26)	FAST	1D-CSI	1.5	15	0.33±0.07
(6)	TRiST	1D-CSI	3	8	0.32±0.07
(7)	TwiST	1D-CSI	3	12	0.33±0.08
(27)	TDST	1D-ISIS	3	15	0.32±0.05
average					0.323±0.067
Skeletal muscle (Calf)					
(6)	TRiST	1D-CSI	3	6	0.26±0.04
(28)	ST	-	3	6	0.31±0.04
(28)	ST	-	7	6	0.35±0.03
(29)	ST	TSE	3	30	0.23-0.29
(30)	Prog. Sat.	TSE	3	23	0.26-0.32
(31)	ST	1D-ISIS	7	23	0.27-0.34
(32)	IT	-	7	10	0.46±0.09
(33)	IT	-	7	7	0.26±0.02
average					0.274±0.041

[1] FAST = four-angle saturation transfer, TRiST = triple repetition time saturation transfer, TwiST = two repetition time saturation transfer, TDST = time-dependent saturation transfer, ST = saturation transfer, Prog. Sat. = progressive saturation, IT = inversion transfer,

[2] CSI = chemical shift imaging, ISIS = image-selected in-vivo spectroscopy, TSE = turbo spin echo.